^{123}I-BZA2 as a Melanin-Targeted Radiotracer for the Identification of Melanoma Metastases: Results and Perspectives of a Multicenter Phase III Clinical Trial

Florent Cachin[1–3], Elisabeth Miot-Noirault[2,3], Brigitte Gillet[4], Vanina Isnardi[5], Bruno Labeille[6], Pierre Payoux[7], Nicolas Meyer[8], Serge Cammilleri[9], Caroline Gaudy[10], Micheline Razzouk-Cadet[11], Jean Philippe Lacour[12], Florence Granel-Brocard[13], Christelle Tychyj[14], Fathalah Benbouzid[15], Jean Daniel Grange[15], Françoise Baulieu[16], Antony Kelly[1], Charles Merlin[1], Danielle Mestas[1], Françoise Gachon[17], Jean Michel Chezal[2,3], Françoise Degoul[2,3], and Michel D'Incan[2–4]

[1]Nuclear Medicine, Jean Perrin Cancer Center, Clermont-Ferrand, France; [2]INSERM, UMR 990, IMTV, Clermont-Ferrand, France; [3]Clermont Université, Université d'Auvergne, IMTV, Clermont-Ferrand, France; [4]Dermatology, Estaing University Hospital, Clermont-Ferrand, France; [5]Nuclear Medicine, University Hospital, Saint-Etienne, France; [6]Dermatology, University Hospital, Saint-Etienne, France; [7]Nuclear Medicine, Purpan University Hospital, Toulouse, France; [8]Dermatology, Larrey University Hospital, Toulouse, France; [9]Nuclear Medicine, La Timone University Hospital, Marseille, France; [10]Dermatology, La Timone University Hospital, Marseille, France; [11]Nuclear Medicine, Archet University Hospital, Nice, France; [12]Dermatology, Archet University Hospital, Nice, France; [13]Dermatology, Brabois University Hospital, Nancy, France; [14]Nuclear Medicine, Lyon Sud University Hospital, Hospices Civils de Lyon, Lyon, France; [15]Ophthalmology, Croix-Rousse University Hospital, Hospices Civils de Lyon, Lyon, France; [16]Nuclear Medicine, Trousseau University Hospital, Tours, France; and [17]Radiopharmacy, Jean Perrin Cancer Center, Clermont-Ferrand, France

Our group has developed a new radiopharmaceutical, ^{123}I-*N*-(2-diethylaminoethyl)-2-iodobenzamide (^{123}I-BZA2), a benzamide derivative able to bind to melanin pigment in melanoma cells. In a prospective and multicentric phase III clinical study, the value of ^{18}F-FDG PET/CT and ^{123}I-BZA2 scintigraphy was compared for melanoma staging. **Methods:** Patients with a past history of cutaneous or ocular melanoma were included from 8 hospitals. ^{18}F-FDG imaging was performed according to a standard PET protocol. Whole-body, static planar, and SPECT/CT (if available) images were acquired 4 h after injection of a 2 MBq/kg dose of ^{123}I-BZA2. ^{18}F-FDG and ^{123}I-BZA2 sensitivity and specificity for the diagnosis of melanoma metastasis were calculated and compared on both a lesion basis and a patient basis. True-positive and true-negative lesion status was determined after 6 mo of clinical follow-up or according to lesion biopsies (if available). Melanin content in biopsies was evaluated with the standard Fontana–Masson silver method and was correlated with ^{123}I-BZA2 uptake. Based on statistical analysis, the number of inclusions was estimated at 186. **Results:** In all, 87 patients were enrolled from 2008 to 2010. Of these, 45 (52%) had metastases. A total of 338 imaging abnormalities were analyzed; 86 lesions were considered metastases, and 20 of 25 lesion biopsies found melanoma metastases. In a patient-based analysis, the sensitivity of ^{18}F-FDG for diagnosis of melanoma metastases was higher than that of ^{123}I-BZA2, at 87% and 39%, respectively ($P < 0.05$). For specificity, ^{18}F-FDG and ^{123}I-BZA2 were not statistically different, at 78% and 94%, respectively. In a lesion-based analysis, the sensitivity of ^{18}F-FDG was statistically higher than that of ^{123}I-BZA2 (80% vs. 23%, $P < 0.05$). The specificity of ^{18}F-FDG was lower than that of ^{123}I-BZA2 (54% vs. 86%, $P < 0.05$). According to biopsy analysis, only 9 of 20 metastatic lesions (45%) were pigmented with high melanin content. ^{123}I-BZA2 imaging was positive for 6 of 8 melanin-positive lesions, fairly positive for 3 of 10 melanin-negative lesions, and negative for 7 of 10 melanin-negative lesions. The sensitivity and specificity of ^{123}I-BZA2 for the diagnosis of melanin-positive lesions were 75% and 70%, respectively. Because of a low ^{123}I-BZA2 sensitivity, this clinical trial was prematurely closed after 87 patients had been included. **Conclusion:** This study confirms the value of ^{18}F-FDG PET/CT for melanoma staging and strengthens the high accuracy of ^{123}I-BZA2 for diagnosis of melanin-positive metastatic melanoma. Moreover, benzamide derivatives radiolabeled with therapeutic radionuclide may offer a new strategy for the treatment of metastatic melanoma patients harboring melanin-positive metastases.

Key Words: melanoma staging; ^{18}FDG; ^{131}I BZA2; melanin; benzamide

J Nucl Med 2014; 55:15–22
DOI: 10.2967/jnumed.113.123554

Melanoma accounts for nearly 80% of all deaths related to cutaneous cancer (*1*). It is the second most common cancer among patients in their second decade (*2*). For localized lesions with a tumor thickness of less than 1.5 mm (stage I or II), melanoma can be cured by total resection, with a 5-y overall survival approaching 90%. Unfortunately, this cancer displays a strong tendency to metastasize. In patients who develop metastasis (stage IV), the median survival rate is around 6–12 mo, and survival at 5 y does not exceed 5% (*3*). However, detection of metastasis has become more pressing since the recent advent of promising drugs such as anti-BRAF (*4*) or T-cell immunostimulant (*5*) agents, with a high response rate and improvement of overall survival.

Usually, melanoma staging involves chest radiography, abdominal sonography, or chest and abdominal CT scanning. MR imaging can be added for specific clinical explorations such as liver,

Received Mar. 24, 2013; revision accepted Jul. 25, 2013.
For correspondence or reprints contact: Cachin Florent, Nuclear Medicine Department, Comprehensive Cancer Center Jean Perrin, 58 rue Montalembert, 63011 Clermont-Ferrand, France.
E-mail: florent.cachin@cjp.fr
Published online Nov. 21, 2013.

cerebral, or soft-tissue melanoma metastasis. Autopsies of patients with known melanoma have revealed more frequent metastases than is regularly clinically reported, indicating that both clinical evaluation and these conventional imaging techniques underestimate the extent of the disease (*6*). PET with ^{18}F-FDG is a functional imaging technique that can reliably visualize malignancy in structures that are still macroscopically normal. In an oncology setting, ^{18}F-FDG PET has become a major clinical diagnostic and prognostic tool that often allows appropriate changes in patient treatment (*7*). However, in many cases, ^{18}F-FDG tracer does not discriminate between inflammatory processes and tumoral lesions. In addition, a PET camera is costly and not available in every nuclear medicine department.

In this context, our group has developed specific SPECT radiopharmaceuticals for malignant melanoma imaging. This approach would be of potential value for the staging and ongoing management of patients. We previously reported on a series of iodobenzamide derivatives that show affinity for melanin (*8*). A first selected compound, *N*-(2-diethylaminoethyl)-4-iodobenzamide (BZA), labeled with ^{123}I, was studied in a phase II clinical trial on 110 patients and showed a sensitivity of 81% and a specificity of 100% (*9*). To optimize the too-long delay between tracer injection and SPECT acquisition (18–24 h after ^{123}I-BZA administration), the orthoiodinated BZA analog ^{123}I-*N*-(2-diethylaminoethyl)-2-iodobenzamide (^{123}I-BZA2), which in preclinical studies had previously demonstrated better imaging contrast than BZA in liver, lung, and brain, organs known to develop melanoma metastases, was also studied in 25 patients in a phase II clinical trial (*10*). After a follow-up of more than 1 y, the overall results of ^{123}I-BZA2 scintigraphy on a per-patient basis showed a sensitivity of 100% and a specificity of 95% (*11*).

Here we report the results of a phase III clinical trial comparing ^{123}I-BZA2 with ^{18}F-FDG PET efficacy for staging or restaging cutaneous or ocular melanoma. The main objective was to compare the specificities of ^{123}I-BZA2 scintigraphy and ^{18}F-FDG PET. The study was initially designed with a large series of patients to address a statistical hypothesis. Unexpected results compelled us to close our study prematurely. However, the final conclusion of our work prefigures new opportunities for melanoma treatment based on melanin-targeted radiopharmaceuticals.

MATERIALS AND METHODS

Patients

This prospective clinical trial was reviewed by the local ethics committee and was performed in accordance with its ethical standards. The study was also reviewed and approved by the French national institutional review board (French National Agency of Drug Safety and Health Product: agreement number 060716). Each included patient gave informed consent in writing.

Patients with a history of cutaneous or ocular melanoma who presented at any of 8 hospitals were prospectively included from 2008 to 2010. The 8 hospitals were the Estaing University Hospital/Jean Perrin Comprehensive Cancer Center, Clermont-Ferrand; Nord University Hospital, Saint-Etienne; Purpan University Hospital, Toulouse; Sainte-Marguerite University Hospital, Marseille; Archet University Hospital, Nice; Fournier University Hospital, Nancy; Croix-Rousse University Hospital, Lyon; and Trousseau University Hospital, Tours. All patients met the following inclusion criteria: age greater than 18 y, negative serum β-subunit human chorionic gonadotropin in potential childbearing women in the 3 d preceding injection of any tracers, Karnofsky index over 70%, life expectancy over 9 mo, and past history of chemotherapy longer than 2 mo. Melanoma status at inclusion was one of the following: newly diagnosed cutaneous or ocular melanoma at any TNM stage, presence of known visceral melanoma metastases, or cutaneous melanoma metastases with unknown primary tumor. Patients with melanoma without metastases were also included, principally to assess the specificity of the imaging. At inclusion, initial staging was performed with a skin and general clinical examination and with imaging techniques usually used for staging, that is, whole-body CT or abdominal sonography. According to personal clinical history, some patients underwent bone scintigraphy and MR imaging.

At the end of this staging procedure, patients were classified into 2 groups: patients with melanoma metastases (M1) and patients in whom no metastases could be demonstrated by conventional techniques (M0).

All patients were reevaluated clinically and by CT scanning at least 6 mo after ^{123}I-BZA2 and ^{18}F-FDG PET imaging.

Imaging Acquisition and Processing

^{18}F-FDG PET/CT and scintigraphy were performed in the 4 wk after pathology staging.

^{123}I-BZA2 Scintigraphy. The synthesis of ^{123}I-BZA2, described previously (*12*), was performed by Cyclopharma Laboratory and MAP Medical and consisted of a simple, reliable isotopic exchange procedure currently used for the ^{125}I-labeling of benzamides. A solution of 5 mg of BZA2 in 0.1 M sodium acetate buffer with a pH of 5 (0.5 mL) was added to 123–296 MBq of ^{123}I-NaI (MAP Medical) obtained by (p, 2n) or (p, pn) reactions. The reaction mixture was heated at 140°C for 50 min. The labeled dry residue was dissolved in 2 mL of NaCl (0.9%). Free iodides were trapped by shaking with 0.2 mL of an anion exchange resin, and the solution was run through a 0.22-μm filter (Millipore) and placed in penicillin-type sterile bottles, ready for intravenous injection. The radiolabeling yield was around 75%, and the specific radioactivity of the final product ranged from 18.5 to 44.4 MBq/mg. Radiochemical purity was at least 95% as controlled by thin-layer chromatography. On the basis of previous pharmacokinetics studies, the whole-body effective dose for a 70-kg patient was estimated to be 0.011 mSv·MBq^{-1} (*11*).

For the imaging procedure, an oral dose of potassium iodide (500 mg) was given to each patient 1 h before radiotracer injection to block thyroid uptake. ^{123}I-BZA2, provided by Cyclopharma (2 MBq/kg; range, 130–185 MBq in 3 mL), was slowly injected intravenously.

Images were acquired 4 h after injection: anterior and posterior whole-body planar images, along with left/right skull profile, anterior/posterior thoracic, anterior/posterior abdominal, and anterior/posterior pelvic 5-mm static views (matrix, 128 × 128). The optimal collimator for ^{123}I acquisition was applied according to the type of camera used. Complementary SPECT or SPECT/CT (when available) imaging was performed according to the results of the planar view. SPECT reconstructions were performed according to local clinical practice (Table 1).

^{18}F-FDG PET. All patients had fasted for 4–6 h before the study but were encouraged to drink water. All patients had blood glucose levels below 10 mmol/L.

Patients received a 3–5 MBq/kg dose of ^{18}F-FDG (GlucoTEP; Cyclopharma). Systematic whole-body PET/CT images were acquired 60 min after injection. Images were processed according to the PET/CT camera used and are summarized in Table 2.

Imaging Qualitative Analysis

The ^{18}F-FDG PET scans were analyzed visually by an experienced nuclear physician who could seek a second opinion from colleagues if there was any doubt about the nature of an abnormality. The PET images were first read independently of the CT images and then were directly correlated with CT abnormalities. An ^{18}F-FDG PET scan was considered positive if at any site there was focal uptake greater than mediastinal or liver uptake that could not clearly be related to physiologic processes. An ^{18}F-FDG PET scan was considered negative when a normal distribution of tracer was observed, even if the CT scan showed

TABLE 1
^{123}I BZA2 SPECT Acquisition Parameters According to Hospital and Camera

Hospital	Camera	Matrix, number of steps, and step duration	Reconstruction method	SPECT/CT
Estaing UH/Jean Perrin CC, Clermont-Ferrand	Axis, Philips, 2 heads	128, 60, 30 s	Filtered backprojection	No
Nord UH, Saint-Etienne	Helix, Elscint, 2 heads	128, 60, 34 s	Filtered backprojection	Yes
Purpan UH, Toulouse	Irix, Philips, 3 heads	128, 120, 30 s	Iterative	No
Sainte-Marguerite UH, Marseille	e.cam 2, Siemens, 2 heads	128, 64, 30 s	Iterative	No
Archet UH, Nice	Infinia, GE, 2 heads	128, 60, 30 s	Iterative	No
Fournier UH, Nancy	Symbia T2, Siemens, 2 heads	128, 64, 30 s	Iterative	Yes
Croix-Rousse UH, Lyon	Symbia T2, Siemens, 2 heads	128, 64, 30 s	Iterative	Yes
Trousseau UH, Tours	Symbia T2, Siemens, 2 heads	128, 60, 30 s	Iterative	Yes

UH = University Hospital; CC = Comprehensive Cancer Center; GE = GE Healthcare.

abnormalities. Bone accumulations were considered positive when the uptake was higher than in normal bone marrow. Any instance of equivocal PET uptake was considered positive.

The ^{123}I-BZA2 scans were analyzed visually by the local nuclear physicians and reviewed centrally by an expert. Any uptake that was more intense than surrounding background tissue was considered to indicate melanoma metastases. Any instance of equivocal uptake was considered positive.

For each patient, lesions detected by ^{18}F-FDG PET or ^{123}I-BZA2 imaging were collected in an electronic database in reference to predefined sites: bone, skin, soft-tissue, supradiaphragmatic lymph node, infradiaphragmatic lymph node, liver, lung, adrenal gland, and brain metastases. Other sites were classified as "other." Five lesions at most per anatomic region were collected.

Imaging Accuracy

Six months after imaging, lesions identified by nuclear physicians were automatically structured, filtered from the database, and presented to the clinicians. Imaging results were compared with clinical evolution, conventional imaging (CT scan), and pathology results when available. Any abnormality visualized on conventional images and considered benign by nuclear physicians was considered true-negative (TN) if it remained stable at 6 mo of follow-up or if biopsy did not demonstrate any metastasis. Imaging abnormalities were considered false-negative (FN) when evidence of disease was found with other diagnostic tools, clinical follow-up, or biopsy or when lesion growth was identified on follow-up. Uptake abnormalities visualized on ^{18}F-FDG PET or ^{123}I-BZA2 imaging were considered true-positive (TP) if distant metastases were detected and confirmed with other diagnostic modalities, clinical follow-up, or biopsy. Finally, false-positive lesions (FP) were defined as abnormalities that were recorded as positive but for which distant metastases remained unconfirmed by other diagnostic tests, clinical follow-up, or biopsy.

Lesion- and patient-based analyses were performed. The sensitivity, specificity, positive predictive value (PPV), negative predictive value (NPV), and accuracy of ^{18}F-FDG PET and ^{123}I-BZA2 imaging for melanoma metastasis detection were then calculated. Sensitivity was defined as TP/(TP + FN), specificity as TN/(TN + FP), PPV as TP/(TP + FP), NPV as TN/(TN + FN), and accuracy as (TP + TN)/(TN + TP + FN + FP).

Whenever possible, biopsies of lesions identified by ^{123}I-BZA2 imaging were processed and slides examined with standard hematoxylin and eosin staining. To demonstrate a potential link between the melanin content of melanoma metastases and positive uptake of ^{123}I-BZA2, pigmentation status was assessed using Fontana–Silver staining and recorded as "pigmented" or "not pigmented."

Statistical Analysis

On the basis of our previous phase II clinical trial (*11*), we hypothesized for ^{123}I-BZA2 a per-patient sensitivity and specificity of 90% and 99.5%, respectively. For ^{18}F-FDG PET we expected respective values of 70% and 94.5%. A 5% specificity difference (99.5–94.5) between the 2 modalities was the main endpoint of our present study. Considering that specificity and sensitivity were calculated on the same population sample, with a 1-sided type I error equal to 0.05 and power equal to 90%, 186 patients were considered necessary to demonstrate this 5% specificity difference.

Sensitivity, specificity, PPV, NPV, and accuracy of ^{18}F-FDG PET and ^{123}I-BZA2 imaging were compared using the χ^2 test. Visual uptake of ^{123}I-BZA2 was correlated with melanin pigmentation of melanoma metastases using the Fisher exact test.

RESULTS

Patients

From August 2008 to September 2010, only 87 of the 186 patients were included because of premature study closure. Patient

TABLE 2
^{18}F-FDG PET/CT Acquisition Parameters According to Hospital and Camera

Hospital	Camera	Injected activity (MBq/kg)	Bed duration (min)	Reconstruction method
Estaing UH/Jean Perrin CC, Clermont-Ferrand	Discovery ST2, GE	5.5	4	Iterative
Nord UH, Saint-Etienne	Biograph 6, Siemens	5.0	3	Iterative
Purpan UH, Toulouse	Biograph HIREZ True Point, Siemens	3	2.4	Iterative
Sainte-Marguerite UH, Marseille	Discovery ST2, GE	4.5	3	Iterative
Archet UH, Nice	Discovery ST4, GE	6	3	Iterative
Fournier UH, Nancy	Biograph 6, Siemens	4	3	Iterative
Croix-Rousse UH, Lyon	Gemini Dual, Philips	4.5	3	Iterative
Trousseau UH, Tours	Gemini, Philips	4.5	3	Iterative

UH = University Hospital; CC = Comprehensive Cancer Center; GE = GE Healthcare.

characteristics are summarized in Table 3. For initial staging, 66 of 87 patients (75.9%) underwent diagnostic CT, 13 (14.9%) underwent abdominal sonography, 8 (9.2%) underwent MR imaging, and 45 (51.7%) were diagnosed with melanoma metastases at inclusion.

Imaging

Of the 87 patients, 75 (86.2%) underwent ^{18}F-FDG PET, 69 (79.3%) ^{123}I-BZA2 scintigraphy, and 69 (79.3%) both. Imaging cancelation resulted principally from delivery and production difficulties.

TABLE 3
Patient and Tumor Characteristics

Characteristic	*n*	%
Patient		
Age (y)		
<50	23	26.4
50–65	36	41.4
>65	28	32.2
Sex		
Male	42	48.3
Female	45	51.7
Hospital		
Estaing UH/Jean Perrin CC, Clermont-Ferrand	18	20.7
Nord UH, Saint-Etienne	18	20.7
Purpan UH, Toulouse	14	16.1
Sainte-Marguerite UH, Marseille	10	11.5
Archet UH, Nice	10	11.5
Fournier UH, Nancy	7	8.0
Croix-Rousse UH, Lyon	6	6.9
Trousseau UH, Tours	4	4.6
Past history of treatment		
None	44	50.6
Chemotherapy	14	16.1
Radiotherapy	2	2.3
Interferon	4	4.6
Not known	23	26.4
Tumor		
Histology		
Ocular melanoma	7	8.0
Nodular melanoma	21	24.1
Superficial spreading melanoma	30	34.5
Acral lentiginous melanoma	6	6.9
Other	6	6.9
Not known	17	19.5
Cutaneous melanoma pigmentation		
Pigmented	51	58.6
Achromic	7	8.0
Not known	29	33.3
Prognosis factor		
Clark level		
I	3	3.4
II	2	2.3
III	20	23.0
IV	46	52.9
V	3	3.4
Not known	13	14.9
Breslow thickness (mm)		
<1.0	12	13.8
1.0–2.0	34	39.1
≥2.0	41	47.1

UH = University Hospital; CC = Comprehensive Cancer Center.

Twenty-two of 69 patients (31.9%) underwent SPECT/CT, the others SPECT alone. The interval between PET and ^{123}I-BZA2 imaging was 5.5 ± 16 d.

In the PET patient group, and after comparison of lesions depicted on imaging with clinical follow-up or biopsies, the final number of patients with metastases was 39 and the number of metastatic lesions was 86.

In the ^{123}I-BZA2 patient group, after comparison of lesions depicted on imaging with clinical follow-up or biopsies, the final number of patients with metastases was 36 and the number of metastatic lesions was 74.

^{18}F-FDG PET Patient-Based Analysis. Of the 75 patients who underwent ^{18}F-FDG PET, 34 (45.3%) were classified as TP, 8 (10.7%) as FP, 20 (26.7%) as TN, and 5 (6.7%) as FN. The sensitivity, specificity, PPV, NPV, and accuracy of ^{18}F-FDG PET for diagnosis of melanoma metastases were 0.87, 0.78, 0.91, 0.85, and 0.83, respectively; in 10 of 37 patients initially classified as M0 at inclusion, melanoma metastases were found on PET.

^{18}F-FDG PET Lesion-Based Analysis. In total, 176 lesions depicted on ^{18}F-FDG PET were analyzed; 110 foci were recorded as positive by the nuclear physician. Of the 176 lesions, 68 (38.6%) were classified as TP, 42 (23.9%) as FP, 49 (27.8%) as TN, and 17 (10.0%) as FN. In the lesion-based analysis, sensitivity for diagnosis of melanoma metastases was 0.80, specificity was 0.54, PPV was 0.66, NPV was 0.74, and accuracy was 0.67.

^{123}I-BZA2 Patient-Based Analysis. Of the 69 patients who underwent ^{123}I-BZA2 scintigraphy, 67 (97.1%) were imaged with SPECT and 3 with SPECT/CT. Nonspecific activity was concentrated mainly in the liver, urinary bladder, and stomach as previously published (*10*).

Of the 67 patients who underwent SPECT or SPECT/CT, 14 (20.9%) were TP, 2 (3.0%) were FP, 31 (46.3%) were TN, and 22 (32.8%) were FN. Sensitivity, specificity, PPV, NPV, and accuracy for diagnosis of melanoma metastases were 0.39, 0.94, 0.88, 0.58, and 0.65, respectively. Sensitivity, NPV, and accuracy were statistically lower for^{123}I-BZA2 imaging than for ^{18}F-FDG PET.

Interpretation was 100% consistent between local and central experts.

^{123}I-BZA2 Lesion-Based Analysis. In total, 162 lesions depicted on ^{123}I-BZA2 scintigraphy were analyzed. Of these, 40 (24.7%) were considered positive by the nuclear physicians. In the final lesion-based analysis, 17 (10.5%) were TP, 12 (7.4%) FP, 76 (46.9%) TN, and 57 (35.2%) FN. The sensitivity, specificity, PPV, NPV, and accuracy of ^{123}I-BZA2 for diagnosis of melanoma metastases were 0.23, 0.86, 0.60, 0.57, and 0.57, respectively. Sensitivity and NPV were statistically lower for ^{123}I-BZA2 than for ^{18}F-FDG. ^{123}I-BZA2 specificity was statistically higher than ^{18}F-FDG specificity. The global performance of imaging is summarized in Tables 4–6.

Interpretation was 100% consistent between local and central experts.

Discordance Between ^{18}F-FDG and ^{123}I-BZA2. Of the TP lesions depicted on ^{18}F-FDG PET, 45 were not visualized on ^{123}I-BZA2 imaging (6 lung, 9 soft-tissue, 10 lymph node, 3 skin, 9 bone, 1 liver, 1 cerebral, 3 adrenal gland, 1 kidney, and 2 others). Five TP lesions seen on ^{123}I-BZA2 were not seen on PET (1 left renal, 1 right axillary lymph node, 1 bone, 1 soft-tissue, and 1 skin).

Eight lesions TN on PET were FP on ^{123}I-BZA2 (3 bone, 1 lung, 1 lymph node, 1 liver, and 2 others); 35 PET FP lesions were not visualized on ^{123}I-BZA2 (9 lymph node, 1 lung, 12 bone, 7 other, 3 soft-tissue, 1 skin, 2 liver).

TABLE 4
^{123}I-BZA2 Performance According to Anatomic Location

Anatomic location	^{123}I-BZA2 lesions (*n*)			
	TP	TN	FN	FP
Bone	2	16	11	3
Skin	3	1	3	1
Soft tissue	3	9	11	0
Supradiaphragmatic lymph node				
Mediastinal lymph node	—	3	3	2
Nonmediastinal lymph node	1	7	8	1
Infradiaphragmatic lymph node				
Inguinal lymph node	2	2	—	1
Noninguinal lymph node	1	3	1	1
Brain	1	2	6	—
Lung	3	15	6	—
Liver	—	6	1	1
Adrenal gland	—	2	3	—
Other	1	10	4	2
Total	17	76	57	12

Biopsy Analysis

A total of 25 biopsies (1 per patient) were performed. Sites of tissue sampling were lung (n = 5), soft tissue (n = 6), lymph nodes (n = 10), liver (n = 1), skin (n = 2), and adrenal glands (n = 1).

Five biopsies had benign results. Twenty showed metastatic tissue, in which only 9 (45%) samples contained melanin pigment.

Among the 20 patients in whom biopsy showed melanoma metastases, only 18 had undergone ^{123}I-BZA2 imaging; 6 of 8 (75%) pigmented lesions were positive for ^{123}I-BZA2 accumulation, 7 of 10 (70%) nonpigmented lesions were negative for ^{123}I-BZA2, and the other 3 (30%) showed low ^{123}I-BZA2 uptake.

Thus, considering low ^{123}I-BZA2 uptake as FP for a pigmented lesion, the sensitivity and specificity of ^{123}I-BZA2 for diagnosis of melanin-pigmented melanoma metastases were 75% (95% confidence interval, 39.9%–92.5%) and 70% (95% confidence interval, 35%–93%), respectively. When low ^{123}I-BZA2 uptake was pooled with absence of ^{123}I-BZA2 uptake, sensitivity and specificity were 70% (95% confidence interval, 39.9%–92.5%) and 100%

TABLE 5
^{18}F-FDG Performance According to Anatomic Location

Anatomic location	^{18}F-FDG lesions (*n*)			
	TP	TN	FN	FP
Bone	12	7	2	13
Skin	6	—	1	2
Soft tissue	12	6	4	3
Supradiaphragmatic lymph node				
Mediastinal lymph node	4	1	1	4
Nonmediastinal lymph node	8	3	2	4
Infradiaphragmatic lymph node				
Inguinal lymph node	3	—	—	3
Noninguinal lymph node	2	3	—	1
Brain	2	2	5	—
Lung	10	15	—	2
Liver	2	5	—	2
Adrenal gland	3	2	0	0
Other	4	5	2	8
Total	68	49	17	42

TABLE 6
Overall Performance of ^{18}F-FDG PET and ^{123}I-BZA Imaging for Diagnosis of Melanoma Metastases

Analysis	Sensitivity	Specificity	PPV	NPV	Accuracy
Per patient					
^{18}F-FDG PET/CT	0.87 [0.76,0.98]	0.78 [0.64,0.91]	0.91 [0.78,0.97]	0.85 [0.64,0.96]	0.83 [0.74,0.91]
^{123}I-BZA2 imaging	0.39 [0.23,0.55]*	0.94 [0.79,0.99]	0.88 [0.61–0.99]	0.58 [0.45,0.71]*	0.65 [0.54–0.76]*
Per lesion					
^{18}F-FDG PET/CT	0.80 [0.71,0.88]	0.54 [0.44,0.63]	0.66 [0.57–0.75]	0.74 [0.63–0.85]	0.67 [0.60–0.74]
^{123}I-BZA2 imaging	0.23 [0.13,0.33]*	0.86 [0.79,0.93]*	0.60 [0.42–0.78]	0.57 [0.49–0.65]*	0.57 [0.50–0.65]

*$P < 0.05$.
Data in brackets are 95% confidence intervals.

(95% confidence interval, 62.1%–100%), respectively. In that case, ^{123}I-BZA2 uptake correlated strongly with melanin pigmentation ($P < 0.001$)

Examples of scintigraphy positive or negative for ^{123}I-BZA2 from patients with biopsies positive or negative for melanin are displayed in Figures 1 and 2, respectively.

DISCUSSION

^{123}I-BZA2 is a new radiopharmaceutical able to bind to intracellular melanin. Several preclinical studies, together with a phase II trial from our group, showed that ^{123}I-BZA2 might prove useful for melanoma staging (*8–11,23*).

In this prospective multicentric phase III study evaluating the clinical relevance and pertinence of imaging with this tracer, we compared the efficacy of ^{18}F-FDG PET and ^{123}I-BZA2 scintigraphy for staging and restaging in 87 patients with or without metastases. The study was initially designed for 186 patients on the basis of preliminary data showing a 90% sensitivity and 99.5% specificity for ^{123}I-BZA2. However, during the study, we observed several patients with obvious metastases that were negative on ^{123}I-BZA2 imaging. For ethical reasons, we therefore prematurely stopped enrolling patients.

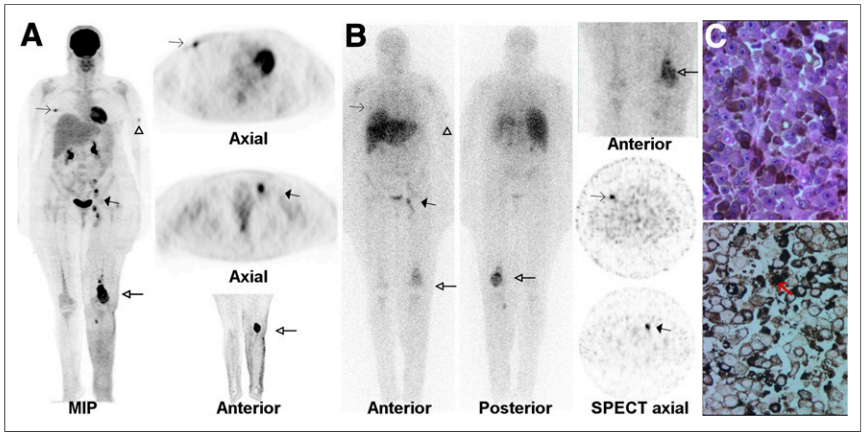

FIGURE 1. A 53-y-old woman with past history of pigmented melanoma of left leg. (A) At inclusion, ^{18}F-FDG PET revealed high-intensity ^{18}F-FDG uptake in right intramammary mass (thin arrows), subcutaneous nodule of left arm (arrowhead), left iliac/femoral lymph node (thick solid arrows), and large left popliteal/femoral/tibial mass (thick open arrows). (B) All lesions were also visualized on ^{123}I-BZA2 planar/whole-body scans and SPECT slices. (C) Standard coloration of popliteal mass biopsy showed melanoma metastases with epithelioid appearance (top). Fontana–Masson coloration (bottom) confirmed high cytoplasmic melanin content (red arrow). MIP = maximum-intensity projection.

At the time this clinical trial was designed, there was no requirement for site certification or a quality control protocol for imaging homogenization. However, all nuclear medicine centers performed acquisitions according to standard guidelines for clinical practice.

Here, we discuss results from 79 of 87 patients imaged with ^{18}F-FDG PET and 69 of 87 imaged with ^{123}I-BZA2 scintigraphy. Because of radiopharmaceutical delivery failure, only 69 patients underwent both imaging examinations. Data analysis restricted to this group did not modify the results (data not shown).

In the patient-based analysis, the sensitivity and specificity of ^{18}F-FDG PET for metastasis detection were 0.87 and 0.78, respectively. These results were consistent with other published data. In a recent metaanalysis based on 2,905 patients, Krug et al. (*13, 14*) reported ^{18}F-FDG PET to have a sensitivity and specificity of 83% and 85%, respectively, at initial staging. In a prospective study of 253 stage III patients, Bastiaannet et al. (*15*) found ^{18}F-FDG PET to have a sensitivity and specificity of 0.86 and 0.93, respectively. However, the clinical question addressed was different in this study from ours, as only patients with stage III candidates for regional lymph node dissection were included. By contrast, in our study most patients had visceral metastases. As has also commonly been reported for other studies, PET changed the initial stage of the disease in 27% of our patients. From the PET results, the stage of 10 patients jumped from stage M0 to stage M1, prompting the clinicians to start active treatment.

Based on lesion analysis, the specificity of ^{18}F-FDG PET in our study was about 0.54—low, compared with values commonly reported. This difference may be because at the outset we considered any equivocal uptake abnormality to represent a metastasis. For instance, 8 PET thyroid foci were analyzed as equivocal by the nuclear physicians and, because of the study rule, were recorded as positive in the database. As expected, these foci were finally found to be FP.

Compared with ^{18}F-FDG, ^{123}I-BZA2 had an unexpectedly low sensitivity (0.39). The performance of ^{123}I-BZA2 was similar regardless of the subgroup of patients studied at inclusion, such as pigmented versus achromic primary melanoma group or

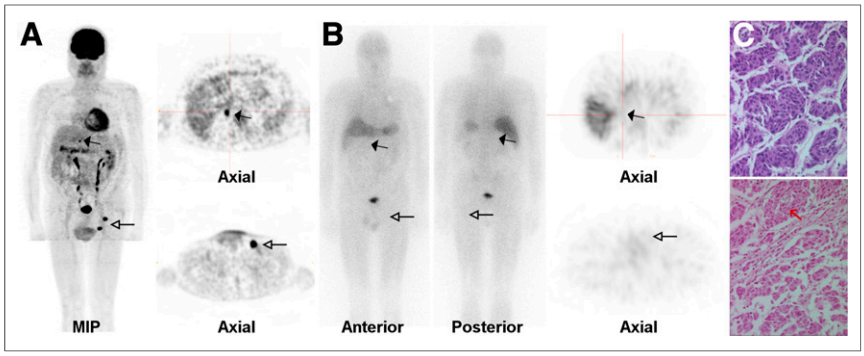

FIGURE 2. A 72-y-old man with history of cutaneous melanoma in 1998. Pigmentation status was unknown. (A) At inclusion, ^{18}F-FDG PET whole-body maximum-intensity projection (MIP) and slices demonstrated intense focal uptake localized in right adrenal gland (solid arrows) and in left iliac lymph node (open arrows). (B) ^{123}I-BZA2 whole-body scans and SPECT slices revealed no tracer accumulation in corresponding lesions. (C) Standard coloration of right adrenal biopsy showed melanoma metastases with fusiform appearance (top). Fontana–Masson coloration (bottom) did not show any intratumoral cytoplasmic melanin pigment (red arrow).

N/N+ group (results not shown). From our experience, positive ^{123}I-BZA2 lesions usually had a high visual contrast ratio independent of tumor size, lesion depth, or site. These arguments suggest that the low sensitivity of ^{123}I-BZA2 was not related only to a lack of SPECT resolution. However, to enhance capacity to detect melanoma metastases, BZA2 PET tracers have to be considered. Similarly, PET radioligands of somatostatin receptor have demonstrated higher accuracy than SPECT tracers in staging of neuroendocrine tumor (*16*). BZA2 could easily be labeled with ^{124}I, a positron emitter isotope of iodine. With higher resolution on PET than SPECT images, ^{124}I-BZA2 will probably be more accurate for staging of melanoma metastases. Nevertheless, some practical limitations lead us to prefer other options, such as the inappropriate half-life of ^{124}I with regard to the BZA2 pharmacokinetic profile; positron energies, which affect spatial resolution; and the risk of high-dose radiation to the patient. In addition, because the synthesis of BZA2 for PET and for SPECT is not directly comparable, the development of pharmaceutical grade ^{124}I-BZA2 would have required costly preclinical and first-in-human validation. Therefore, we turned our attention, as others have (*17*), to ^{18}F-labeled BZA2 analogs. Particularly, we demonstrated in preclinical studies the potential of ^{18}F-*N*-[2-(diethylamino)ethyl]-6-fluoropyridine-3-carboxamide for PET imaging of melanoma (*18*), a use that is under evaluation by Hicks et al. in an ongoing clinical trial (*19*).

Other explanations or work limitations could account for the lower performance of ^{123}I-BZA2 than of ^{18}F-FDG. The biodistribution of ^{123}I-BZA2 typically shows in the liver high physiologic uptake, which certainly decreases the ability to detect liver metastases. In this trial, 1 liver lesion was not detected on ^{123}I-BZA2 images. From a methodologic point of view, only 22 of 68 patients underwent SPECT/CT, although this fact cannot be responsible for the low ^{123}I-BZA2 sensitivity. In 2002 our laboratory reported the results of our first phase II trial, which demonstrated high sensitivity and specificity for ^{123}I-BZA2: 100% and 95%, respectively. Possible sources for such differences could be the design of the study (a monocentric trial, which usually enhances results), differences in inclusion criteria, and the choice of CT as the gold standard, which does not perform as well as ^{18}F-FDG PET for this clinical indication.

Finally, we assume that the low ^{123}I-BZA2 sensitivity is ascribable, in large part, to the high percentage of amelanotic melanoma metastases, as confirmed by biopsy analysis (55%).

Several previously published studies have similarly demonstrated a high incidence of nonpigmented or only slightly pigmented metastases, even in cases of pigmented primary tumors. This question has been extensively assessed in validation processes for new antibodies and for MR imaging diagnosis of melanoma metastases. Perry et al. (*20*) have reviewed a series of 174 fine-needle biopsies of metastatic melanoma. Intracellular melanin in neoplastic cells was absent in 60% of patients. Also, Saqi et al. (*21*) reported the results of 165 fine-needle aspirations from melanoma metastases in 152 patients. Only 56 of the samples (32%) contained melanin. The authors noted that the prevalence of pigment in the specimens varied from focal in many cases to diffuse in some. Melanin content was also evaluated in studies aimed at correlating T1-weighted MR imaging hyperintensity of melanoma lesions with pigmentation. In this context, pigmented lesions were observed in about 50% of patients (*22,23*). Most pigmented samples corresponded to positive ^{123}I-BZA2 scintigraphy results with a visually high ratio of background to tumor. Two pigmented metastases (a left axillary node and a right leg cutaneous metastasis) were not visualized on ^{123}I-BZA2 images, and the lesion size was below 1 cm in each case. Three nonpigmented metastases showed slight ^{123}I-BZA2 uptake, possibly in relation to heterogeneous melanin distribution in metastases. Finally, these data confirm that the tumor accumulation of ^{123}I-BZA2 clearly correlates with melanin content, as previously demonstrated (*15,16*). Therefore, despite the low number of available biopsies, our results suggest that ^{123}I-BZA2 could be used as an accurate radiopharmaceutical for the diagnosis of only pigmented melanoma metastases. However, given the high proportion of achromic metastases in the natural evolution of the disease, no diagnostic tracer targeting melanin, such as ^{123}I-BZA2, can yet challenge ^{18}F-FDG for overall melanoma staging. Therefore, we have stopped any research development for a diagnostic SPECT tracer and have focused our research on therapeutics (*24*). Indeed, the concept of melanin targeting holds promise for therapeutic purposes (*25*). Melanin-targeted imaging could be the first step in selecting patients with pigmented metastases, allowing them to become candidates for targeted therapy. Along with others (*26,27*), we are developing melanin-targeted radiopharmaceuticals dedicated to melanoma treatment based on a quinoxaline derivative, ICF01012, which in preclinical models has demonstrated promising antitumoral activity after labeling with ^{131}I (*28*). This tracer was recently selected for a first-in-human clinical trial to determine tolerance, distribution, and dosimetry in patients with metastatic melanoma. Although this melanin-targeted therapy would concern only patients with pigmented metastasis, it is worth exploration since even commercially available targeted treatments, such as vemurafenib for BRAF mutated melanoma, are available for less than 50% of patients. This treatment, being a new theranostic concept, reflects modern oncology.

CONCLUSION

Our study compared ^{18}F-FDG PET/CT and ^{123}I-BZA2 imaging for staging and restaging of melanoma patients, most of whom

were at stage IV at inclusion. As expected, ^{18}F-FDG PET/CT confirmed a potential value for melanoma staging. We also demonstrated that melanin-targeted tracers such as ^{123}I-BZA2 can identify patients with pigmented metastases. However, because of the interpatient variability of melanoma metastasis pigmentation, such a tracer would probably not be relevant clinically. In view of these results, our research group is investigating new approaches using iodobenzamide derivatives labeled with ^{131}I for the treatment of preselected patients harboring melanin-positive metastases. Such a targeted radionuclide therapy approach could open new prospects for theranostic and personalized medicine in patients with disseminated melanoma.

DISCLOSURE

The costs of publication of this article were defrayed in part by the payment of page charges. Therefore, and solely to indicate this fact, this article is hereby marked "advertisement" in accordance with 18 USC section 1734. This clinical trial was financially supported by the French National Cancer Institute and the French Dermatology Society. Cyclopharma Laboratory provided ^{18}F-FDG and ^{123}I-BZA2 radiopharmaceuticals. No other potential conflict of interest relevant to this article was reported.

ACKNOWLEDGMENTS

We greatly thank Prof. Jean Claude Madelmont, Prof. Annie Veyre, Dr. Nicole Moins, and Dr. Jacques Bonafous for their significant contribution to the development and validation of ^{123}I-BZA2.

REFERENCES

1. Gray-Schopfer V, Wellbrock C, Marais R. Melanoma biology and new targeted therapy. *Nature.* 2007;445:851–857.
2. MacKie RM, Hauschild A, Eggermont AM. Epidemiology of invasive cutaneous melanoma. *Ann Oncol.* 2009;20(suppl 6):vi1–vi7.
3. Finn L, Markovic SN, Joseph RW. Therapy for metastatic melanoma: the past, present, and future. *BMC Med.* 2012;10:23.
4. Sosman JA, Kim KB, Schuchter L, et al. Survival in BRAF V600-mutant advanced melanoma treated with vemurafenib. *N Engl J Med.* 2012;336:707–714.
5. Hodi FS, O'Day SJ, McDermott DF, et al. Improved survival with ipilimumab in patients with metastatic melanoma. *N Engl J Med.* 2010;363:711–723.
6. Leiter U, Meier F, Schittek B, Garbe C. The natural course of cutaneous melanoma. *J Surg Oncol.* 2004;86:172–178.
7. Blodgett TM, Meltzer CC, Townsend DW. PET/CT: form and function. *Radiology.* 2007;242:360–385.
8. Michelot JM, Moreau MF, Labarre PG, et al. Synthesis and evaluation of new iodine-125 radiopharmaceuticals as potential tracers for malignant melanoma. *J Nucl Med.* 1991;32:1573–1580.
9. Michelot JM, Moreau MF, Veyre AJ, et al. Phase II scintigraphic clinical trial of malignant melanoma and metastases with iodine-123-N-(2-diethylaminoethyl 4-iodobenzamide). *J Nucl Med.* 1993;34:1260–1266.
10. Labarre P, Papon J, Moreau MF, Moins N, Veyre A, Madelmont JC. Evaluation in mice of some iodinated melanoma imaging agents using cryosectioning and multi-wire proportional counting. *Eur J Nucl Med.* 1999;26:494–498.
11. Moins N, D'Incan M, Bonafous J, et al. ^{123}I-N-(2-diethylaminoethyl)-2-iodobenzamide: a potential imaging agent for cutaneous melanoma staging. *Eur J Nucl Med Mol Imaging.* 2002;29:1478–1484.
12. Moreau MF, Michelot J, Papon J, et al. Synthesis, radiolabeling, and preliminary evaluation in mice of some (N-diethylaminoethyl)-4-iodobenzamide derivatives as melanoma imaging agents. *Nucl Med Biol.* 1995;22:737–747.
13. Krug B, Pirson AS, Crott R, Vander Borght T. The diagnostic accuracy of ^{18}F-FDG PET in cutaneous malignant melanoma. *Eur J Nucl Med Mol Imaging.* 2010;37:1434–1435.
14. Krug B, Crott R, Lonneux M, Baurain JF, Pirson AS, Vander Borght T. Role of PET in the initial staging of cutaneous malignant melanoma: systematic review. *Radiology.* 2008;249:836–844.
15. Bastiaannet E, Uyl-de Groot CA, Brouwers AH, et al. Cost-effectiveness of adding FDG-PET or CT to the diagnostic work-up of patients with stage III melanoma. *Ann Surg.* 2012;255:771–776.
16. Srirajaskanthan R, Kayani I, Quigley AM, Soh J, Caplin ME, Bomanji J. The role of ^{68}Ga-DOTATATE PET in patients with neuroendocrine tumors and negative or equivocal findings on ^{111}In-DTPA-octreotide scintigraphy. *J Nucl Med.* 2010;51:875–882.
17. Denoyer D, Greguric I, Roselt P, et al. High-contrast PET of melanoma using ^{18}F-MEL050, a selective probe for melanin with predominantly renal clearance. *J Nucl Med.* 2010;51:441–447.
18. Rbah-Vidal L, Vidal A, Besse S, et al. Early detection and longitudinal monitoring of experimental primary and disseminated melanoma using [^{18}F]ICF01006, a highly promising melanoma PET tracer. *Eur J Nucl Med Mol Imaging.* 2012; 39:1449–1461.
19. A phase 0 exploratory microdosing study of 6-18fluoro-N-[2-(diethylamino) ethyl]pyridine-3-carboxamide (^{18}F MEL050) using PET/CT in patients with metastatic melanoma. ClinicalTrials.gov Web site. Identifier, NCT01620749. http://clinicaltrials.gov/ct2/show/study/NCT01620749. Published May 27, 2012. Updated June 14, 2012. Accessed October 30, 2013.
20. Perry MD, Gore M, Seigler HF, Johnston WW. Fine needle aspiration biopsy of metastatic melanoma: a morphologic analysis of 174 cases. *Acta Cytol.* 1986;30:385–396.
21. Saqi A, McGrath CM, Skovronsky D, Yu GH. Cytomorphologic features of fine-needle aspiration of metastatic and recurrent melanoma. *Diagn Cytopathol.* 2002; 27:286–290.
22. Gaviani P, Mullins ME, Braga TA, et al. Improved detection of metastatic melanoma by T2*-weighted imaging. *AJNR.* 2006;27:605–608.
23. Ghanem N, Altehoefer C, Högerle S, et al. Detectability of liver metastases in malignant melanoma: prospective comparison of magnetic resonance imaging and positron emission tomography. *Eur J Radiol.* 2005;54:264–270.
24. Ren G, Pan Y, Cheng Z. Molecular probes for malignant melanoma imaging. *Curr Pharm Biotechnol.* 2010;11:590–602.
25. Dadachova E, Casadevall A. Renaissance of targeting molecules for melanoma. *Cancer Biother Radiopharm.* 2006;21:545–552.
26. Ballard B, Jiang Z, Soll CE, et al. In vitro and in vivo evaluation of melanin-binding decapeptide 4B4 radiolabeled with ^{177}Lu, ^{166}Ho, and ^{153}Sm radiolanthanides for the purpose of targeted radionuclide therapy of melanoma. *Cancer Biother Radiopharm.* 2011;26:547–556.
27. Joyal JL, Barrett JA, Marquis JC, et al. Preclinical evaluation of an ^{131}I-labeled benzamide for targeted radiotherapy of metastatic melanoma. *Cancer Res.* 2010; 70:4045–4053.
28. Bonnet-Duquennoy M, Papon J, Mishellany F, et al. Targeted radionuclide therapy of melanoma: anti-tumoural efficacy studies of a new ^{131}I labelled potential agent. *Int J Cancer.* 2009;125:708–716.